Journal of Colloid and Interface Science 448 (2015) 257–264

Contents lists available at ScienceDirect

Journal of Colloid and Interface Science

www.elsevier.com/locate/jcis

Detection of DNA utilizing a fluorescent reversible change of a biosensor based on the electron transfer from quantum dots to polymyxin B sulfate

Linlin Wang [a], Shaopu Liu [a], Wanjun Liang [a], Dan Li [a], Jidong Yang [a,b], Youqiu He [a,*]

[a] Key Laboratory on Luminescence and Real-Time Analysis, Ministry of Education, School of Chemistry and Chemical Engineering, Southwest University, Chongqing 400715, PR China
[b] School of Chemical and Environmental Engineering, Chongqing Three Gorges University, Chongqing, Wanzhou 404000, PR China

GRAPHICAL ABSTRACT

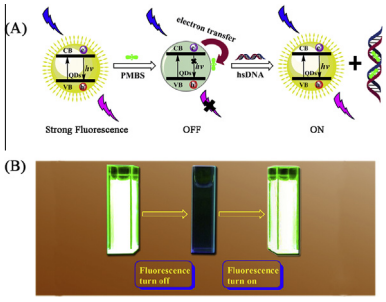

ARTICLE INFO

Article history:
Received 4 December 2014
Accepted 12 February 2015
Available online 23 February 2015

Keywords:
Quantum dots
Polymyxin B sulfate
Herring sperm DNA
Fluorescence
Detection

ABSTRACT

A fluorescent "turn off–on" pattern for the detection of herring sperm DNA (hsDNA) had been designed through utilizing the interaction between polymyxin B sulfate (PMBS) and hsDNA as an inherent performance and the fluorescent transformation of glutathione (GSH)-capped CdTe quantum dots (QDs) as an external manifestation. Due to the occurrence of the photoinduced electron transfer from the QDs to PMBS, the fluorescence of GSH-capped CdTe QDs could be effectively quenched by PMBS, causing the system into "off" state. With the addition of hsDNA, the quenched fluorescence of GSH-capped CdTe QDs could be restored for the reason that PMBS embedded into hsDNA double helix structure to form new complex and peeled off from the surface of GSH-capped CdTe QDs, leading the system into "on" condition. Corresponding experimental results illustrated that the relative recovered fluorescence intensity of GSH-capped CdTe QDs–PMBS system was near proportional to the concentration of hsDNA within the range of 0.059–15.0 μg mL^{-1}. This proposed method demonstrated a good linear correlation coefficient of 0.9937 and a detection limit (3 σ/K) of 0.018 μg mL^{-1} for hsDNA. This dual-directional fluorescent biosensor overcame the selectivity problem commonly existed in the traditional mono-directional fluorescence detection mode and owned perfect analysis applications in biochemical DNA monitoring.

1. Introduction

Deoxyribonucleic acid (DNA) plays an extremely important role in the process of human life, which serving as the carrier of genetic information and gene expression of the material basis. The development of novel effective probes for the detection of DNA and the interactions of drugs with DNA have been the focuses, on account of they may be conducive to realizing the effective mechanism of drugs and the design of new specific DNA-targeted drugs [1–3]. DNA with their evenly stacked base pairs and shallow (minor) and deep (major) grooves are attractive targets for some

* Corresponding author. Fax: +86 23 68254000.
E-mail address: heyq@swu.edu.cn (Y. He).

http://dx.doi.org/10.1016/j.jcis.2015.02.034
0021-9797/

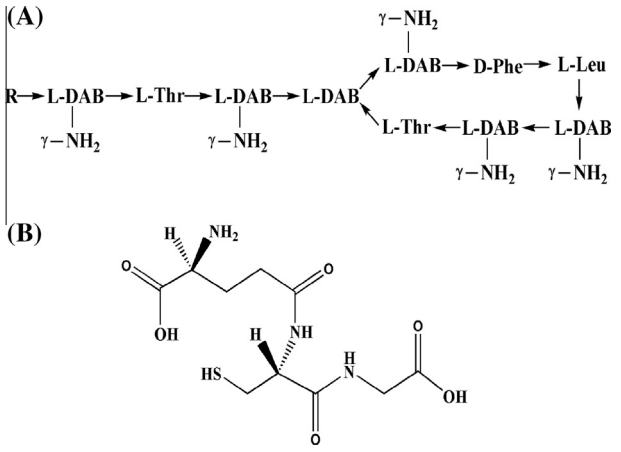

Fig. 1. Chemical structures of (A) polymyxin B (DAB, α, λ-diaminobutyric acid; Thr, threonine; Phe, phenylalanine; Leu, leucine) and (B) glutathione.

drug molecules. The interaction between DNA and drug can cause changes to the structure of DNA, thereby affecting the function of gene-specific regulation and expression in pharmacological activity. Several methods for detection trace amounts of DNA have been established, including fluorescence [4], chemiluminescence [5], electrochemistry [6], and so on. Among them, fluorescence based analytical method are used extensively for its handy, rapid, selective, and the reagents are easily obtainable.

Polymyxin B sulfate (PMBS, molecular structure given in Fig. 1(A)) is an antibiotic widely used in the treatment of infections caused by gram-negative bacteria, which is due to its stronger antibacterial capacity. Previous researches have shown that PMBS, it by itself contains two Thr-OH and five DAB with carbonyl group, can invade lipoprotein through the molecule lipophilic groups and damage the shielding effect of the cell plasma membrane, causing the huge loss of cell sap and the bactericidal effect [7,8]. Nevertheless, whether it can combine with DNA and affect the structure of DNA still unclear.

Among the rich family of inorganic nano-scale building blocks, quantum dots (QDs) attract the attentions of many researchers in recent years. QDs have unique functional and structural properties, such as small size, large absorption cross sections, narrow and Gaussian emission spectra, size- and composition-tunable emission and high photobleaching threshold [9,10]. All of these properties provide important advantages for QDs becoming excellent candidates in the development of novel and sensitive sensors in current researches. Earlier studies related to the interactions of QDs with some compounds have revealed that the interactions make a profound effect on the photophysical properties of QDs [11,12].

While more and more researches have been focusing on the exploration of QDs utilized as fluorescent "turn-off" sensors, very few studies about QDs-based fluorescent "turn off–on" sensors are reported [13,14]. For example, Fang et al. developed a graphene oxide (GO)-based multicolor fluorescent "turn-off" probe to detect DNA targets in homogeneous solution which was depending on the interaction between GO and DNA molecules [15]. Since a variety of factors rather than analytes can induce the ultimate fluorescence "off" state, a fluorescent "turn off–on" model is designed to overcome this problem and effectively lessen the chance of false judgment. Meanwhile, this "turn off–on" pattern is amenable to complex situations, for instance, the simultaneous exclusively detections of sorts analytes [16]. In this study, we had realized a new fluorescent sensor to detect hsDNA (herring sperm DNA) based on the reversible "off–on" fluorescence change of GSH capped-CdTe QDs. PMBS was utilized as it could efficiently quench the high fluorescence of GSH capped-CdTe QDs which causing the system into "off" state. This approach was relied on the electrostatic interaction between the oppositely charged substances of PMBS and GSH-capped CdTe QDs, giving rise to the electron transfer from the photoexcited QDs to PMBS. On the other hand, the high affinity of PMBS to hsDNA enabled PMBS to intercalate into the hsDNA double helix structure and peel off from the surface of GSH-capped CdTe QDs. Therefore, this intercalation reaction hindered the proceeding of the electron transfer from the QDs to PMBS, while recovering the fluorescence of the QDs and leading the system into "on" condition. The principle of this designed fluorescent biosensor for the determination of hsDNA was illustrated in Scheme 1. This dual-directional regulation fluorescence mode of GSH-capped CdTe QDs resolved the selectivity problem existing in traditional mono-directional fluorescence detections. Since it required no modification or coupling of QDs, the drug molecular and DNA were all under the original state, the developed fluorescent "turn off–on" biosensor exhibited the advantages of fast, simple, sensitive and selective for hsDNA monitoring.

2. Materials and methods

2.1. Apparatus

A Hitachi F-2500 fluorospectrophotometer (Tokyo, Japan) was used for measuring the fluorescence with the excitation wavelength of 350 nm and the scattering intensities. The absorption spectra were recorded by making use of a UV-2450 spectrophotometer (Tianmei Corporation, Shanghai, China). JEOL JEM-2100 transmission electron microscopy (TEM, Hitachi, Japan) was used to observe the appearance and size of quantum dots. The ZF-5 Portable UV analyzer was available to observe the fluorescence intensity change of the reaction system under open-air condition (Jiapeng Corporation, Shanghai, China). The pH values of the aqueous solutions were measured though utilizing a PHS-3C pH meter (Leici, Shanghai, China).

2.2. Materials and reagents

In present study, the main chemical reagents adopted were $CdCl_2{\cdot}2.5H_2O$ (Shanghai Chemicals Reagent Co., Shanghai, China), tellurium (Te) powder (Sinopharm Chemical Reagent Co., Shanghai, China), $NaBH_4$ (Tianjin Huanwei Fine Chemical Co., Tianjin, China). Glutathione (GSH) and all of the amino acids used in this paper were purchased from Aladdin Reagent Co. (Shanghai, China). Herring sperm DNA (hsDNA), yeast ribonucleic acid (RNA), bovine serum albumin (BSA), glucose, urea and collagen were obtained from Sigma (St. Louis, MO, USA). The solutions were buffered with Tris–HCl buffer solution, which was prepared by dissolving 0.1 M HCl and 0.1 M tromethamine (Tris) solution together in certain percentage. Unless stated, all reagents used were of analytical grade without further purification. Deionized distilled water prepared from a water purification machine was used throughout.

2.3. Synthesis of GSH-capped CdTe QDs

Aqueous colloids of GSH-capped CdTe QDs solution were prepared according to the previously described methods [17]. Under Ar atmosphere and magnetic stirring, Te powder (0.0383 g) was reacted with excessive sodium borohydride in deionized water to produce the colorless solution of sodium hydrogen telluride (NaHTe). $CdCl_2{\cdot}2.5H_2O$ (0.1028 g) and GSH (0.1844 g) were dissolved in 150 mL deionized water. With the slow Ar flow and vigorous stirring, the pH of the mixture was adjusted to 10.5 by using the dropwise addition of NaOH solution (1.0 M). The solution was

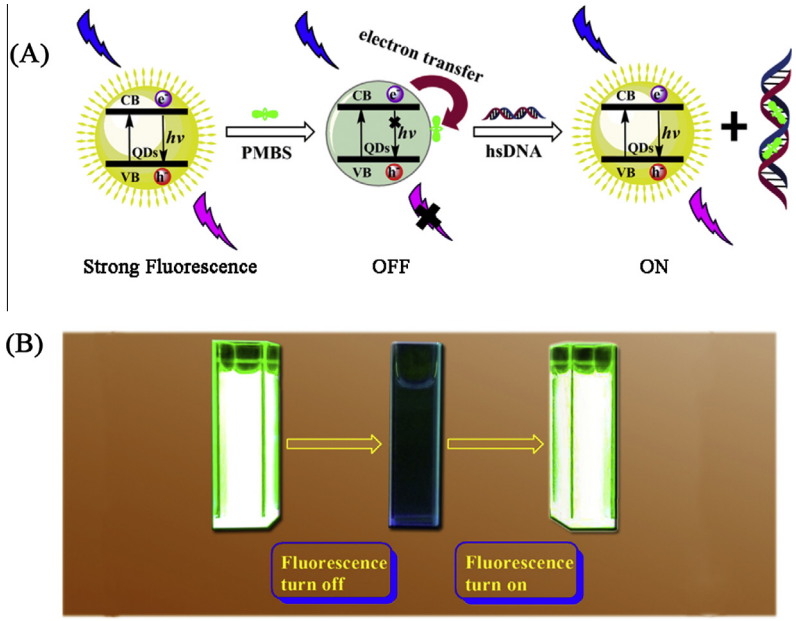

Scheme 1. (A) Schematic illustration of the proposed GSH-capped CdTe QDs–PMBS system based biosensor for detecting hsDNA. (B) Photograph of the corresponding fluorescent "turn off–on" reversible change of the biosensor under UV light at the same time (GSH-capped CdTe QDs, 2.0×10^{-4} M; PMBS, 14.0 μg mL^{-1}; hsDNA, 10.0 μg mL^{-1}).

deaerated by Ar bubbling for about thirty minutes. Under stirring, H_2Te gas generated by the reaction of the solution of NaHTe with diluted H_2SO_4 (0.5 M) was passed through the oxygen-free Cd^{2+} solution together with the slow Ar flow. Then the resulting solution mixture was heated to 369 K and refluxed for one hour under open-air condition with condenser. The salmon pink CdTe solution was obtained. Finally, the concentration of CdTe QDs was 2.0×10^{-3} M (determined by the Te^{2-} concentration) [18].

2.4. Analytical procedure

1.0 mL as-prepared GSH-capped CdTe QDs, 1.0 mL Tris–HCl buffer solution (pH = 7.2) and an appropriate amount of PMBS were dispersed in a 10 mL volumetric flask, then diluted with deionized water to the mark. Each increment of the added PMBS concentration (c_{PMBS}) was from 0 to 14.0 μg mL^{-1}. These samples were used for investigating the fluorescence quenching phenomenon. In addition, the mixture of GSH-capped CdTe QDs and PMBS (14.0 μg mL^{-1}) was applied to analyze the fluorescence enhancement phenomenon of the solution by the introduction of hsDNA. The concentration range of hsDNA (c_{hsDNA}) was from 0 to 15.0 μg mL^{-1}. Furthermore, these two stage analysis processes all needed incubation for ten minutes at room temperature to obtain final fluorescence intensity. The resulting solutions were studied by means of TEM, fluorescence (FL), ultraviolet–visible (UV–vis) absorption and resonance rayleigh scattering (RRS).

3. Results and discussion

3.1. Characterization of the synthesized GSH-capped CdTe QDs

The TEM image which revealed the morphology and diameter of the aqueous GSH-capped CdTe QDs was shown in Fig. 2(A). It was quite evident that the nanoparticles' shapes were approximately spherical and the sizes were uniform in diameter of about 3 nm. Meanwhile, it was also reasonable to analyze the UV–vis absorption and FL emission spectra of GSH-capped CdTe QDs. As shown in Fig. 2(B), the characteristic absorption peak of GSH-capped CdTe QDs was located at 520 nm and the excitonic absorption was strong (curve a). Since QDs had the property of size- and composition-tunable emission, the excitation wavelength of 350 nm was chose to obtain the apparent spectrum. Under the condition of excitation wavelength of 350 nm, the fluorescence spectrum of GSH-capped CdTe QDs (curve b) demonstrated that the full width half maximum (FWHM, about 62 nm) was narrow and exhibiting good symmetry, and the investigated fluorescence band was centered at 554 nm.

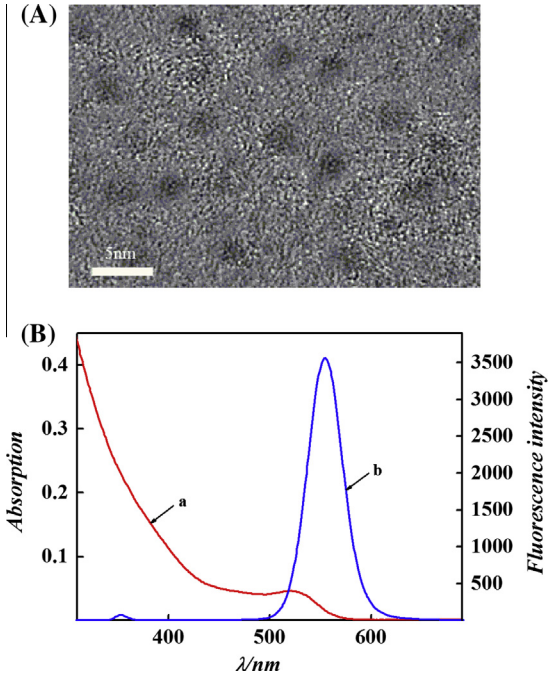

Fig. 2. (A) TEM image, (B) UV–vis absorption (a) and fluorescence spectra (b) of GSH-capped CdTe QDs dispersed in water.

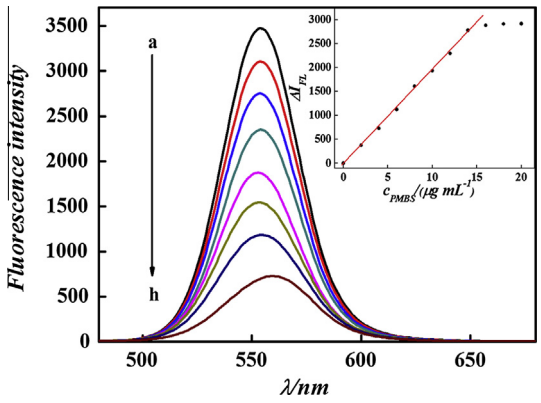

Fig. 3. Fluorescence spectra of GSH-capped CdTe QDs in the absence and presence of PMBS in Tris–HCl buffer solution (pH 7.2, 0.1 M), the concentration of PMBS was (μg mL^{-1}, curves a–h): 0, 2.0, 4.0, 6.0, 8.0, 10.0, 12.0 and 14.0, separately; the inset revealed the relationship between the quenched fluorescence intensity of the QDs and the concentration of PMBS (0, 2.0, 4.0, 6.0, 8.0, 10.0, 12.0, 14.0, 16.0, 18.0 and 20.0 μg mL^{-1}).

The measurement of fluorescence quantum yield (QY) was a key step in the characterization of photoluminescent GSH-capped CdTe QDs, for the reason that it provided a direct measure for the efficiency of the conversion of absorbed photons into emitted photons [19]. The QY of GSH-capped CdTe QDs which was calculated by utilizing the following equation with rhodamine 6G (QY = 95%) as a criterion was about 54.5%.

$$Y_u = Y_s \times \left(\frac{F_u}{F_s}\right) \times \left(\frac{A_s}{A_u}\right) \times \left(\frac{n_u^2}{n_s^2}\right) \quad (1)$$

The subscripts *u* and *s* refer to the referential and standard substances respectively. Y_u was the QY of the unknown solution to be measured while Y_s was the reference sample. *F* denoted the integral intensity, *A* represented the absorption values, and *n* was the refractive coefficient of solvent.

3.2. PMBS as an excellent quencher to GSH-capped CdTe QDs: "turn-off" process

Under the optimum conditions, the fluorescence emission spectra of GSH-capped CdTe QDs were recorded in the absence and presence of PMBS with varying concentrations (0–20.0 μg mL^{-1}), as shown in Fig. 3. Obviously, the fluorescence quenching extent of GSH-capped CdTe QDs was directly proportional to the concentration of PMBS from 0 to 14.0 μg mL^{-1}. When the concentration of PMBS was above 14.0 μg mL^{-1}, corresponding fluorescence intensity variation of the system was almost remained unchanged (shown in the inset of Fig. 3). Videlicet, the concentration of PMBS at 14.0 μg mL^{-1} could cause the fluorescence quenching degree of GSH-capped CdTe QDs to reach a limit. Meanwhile, by comparison, the maximum emission wavelength (λ_{max}) of GSH-capped CdTe QDs presented a 9 nm red shift (from 554 to 563 nm). It was to be proposed that there indeed existed a reaction between GSH-capped CdTe QDs and PMBS, causing the quenching of the fluorescence emission of the QDs [20].

Fluorescence quenching mechanisms are commonly divided into two categories, static quenching and dynamic quenching. Earlier studies have demonstrated that static quenching is due to the formation of non-luminous complex while dynamic quenching results from collision between quenching agent and fluorophor [21]. On the basis of their differing dependence on temperature, static quenching and dynamic quenching can be distinguished. The quenching constants decrease with the increasing temperature for static quenching, whereas the revers effect is observed in case of dynamic quenching [22]. The fluorescence quenching mechanism of the GSH-capped CdTe QDs–PMBS system could be explored by the well-known Stern–Volmer equation [23]:

$$F_0/F = 1 + K_{Sv}[Q] \quad (2)$$

F_0 and *F* were respectively the fluorescence intensities of GSH-capped CdTe QDs in the absence and presence of the quencher (PMBS), [Q] was the concentration of PMBS, and K_{sv} was the Stern–Volmer quenching constant. Eq. (2) was applied to describe the linear regression Stern–Volmer plots of F_0/F against [Q] at the temperatures of 289 K, 296 K and 303 K (as shown in Fig. 4). And the diverse values of K_{sv} at various temperatures were listed in Table 1. Obviously, the values of K_{sv} were decreased with the increasing temperatures, indicating that the possible quenching mechanism was static quenching rather than dynamic quenching. The results indirectly demonstrated the formation of GSH-capped CdTe QDs–PMBS complex, as well.

UV–vis absorption spectroscopy of this system was analyzed to investigate the change of molecular structure and to facilitate understanding of the complex formation. As illustrated in Fig. 5, in the spectrum of pure GSH-capped CdTe QDs (curve a), there existed strong absorption in the UV at the wavelength range of less than 400 nm, whereas the absorption in the visible was relatively weak. By comparing the absorption spectrum of PMBS with distilled water as the reference (curve b) and the absorption spectrum of PMBS with GSH-capped CdTe QDs as the reference (curve d), an obviously spectral change of absorbance was presented. It indicated that there was a strong interaction between GSH-capped CdTe QDs and PMBS, indicating the generation of a new complex. Namely, the quenching type of this system was static quenching.

To clarify the mechanism further, the RRS spectra of GSH-capped CdTe QDs–PMBS system was investigated. RRS is an absorption–rescattering process produced by the resonance between the Rayleigh scattering and the light absorption with the same frequency when the wavelength of Rayleigh scattering

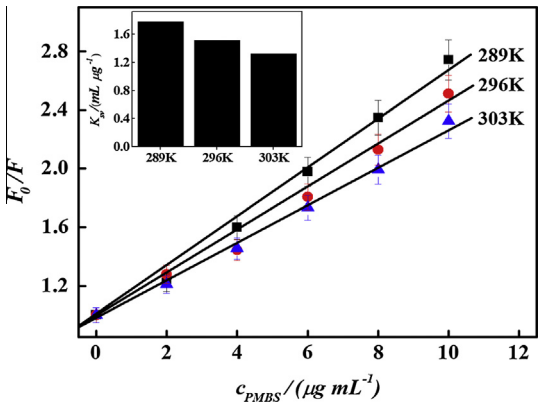

Fig. 4. Stern–Volmer curves for the GSH-capped CdTe QDs–PMBS solution system at three different temperatures in Tris–HCl buffer solution (pH 7.2, 0.1 M).

Table 1
Stern–Volmer quenching constants for the GSH-capped CdTe QDs–PMBS solution system at different temperatures in Tris–HCl buffer solution (pH 7.2, 0.1 M).

Temperature (K)	Sterm–volmer linear equation	K_{sv} (L mol^{-1})	R^a	S.D.[b]
289	F_0/F = 0.9238 + 1.7809 [Q]	1.7809	0.9972	0.0555
296	F_0/F = 0.9566 + 1.5113 [Q]	1.5113	0.9933	0.0733
303	F_0/F = 0.9576 + 1.3208 [Q]	1.3208	0.9976	0.0382

[a] *R* is the correlation coefficient.
[b] S.D. is the standard deviation for the K_{sv} values.

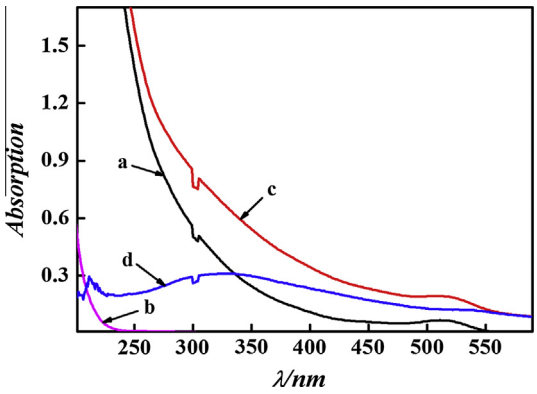

Fig. 5. UV–vis absorption spectra of (a) GSH-capped CdTe QDs, (b) PMBS (with distilled water as the reference), (c) the mixture solution (GSH-capped CdTe QDs and PMBS) and (d) PMBS (with GSH-capped CdTe QDs as the reference), (GSH-capped CdTe QDs, 2.0×10^{-4} M; PMBS, 10.0 μg mL^{-1}).

is located at its absorption band [24]. According to Figs. 2(B) and 6(A), the contrast between the absorption spectrum of GSH-capped CdTe QDs and the RRS spectra of QDs–PMBS system indicated that the peaks located at 380 nm and 550 nm were situated in its absorption band, resulting in the enhancement of resonance scattering. As shown in Fig. 1(B), glutathione (GSH) is a thiol-containing oligopeptide which molecule contains one amino group and two carboxylate groups. Thereby, it is used as a stabilizer for the surface stabilization of CdTe nanocrystals to coate on QD surfaces and provides surface passivation while maintaining its hydrophilic capability. Since GSH is prone to thermal decomposition during the synthesis, most of the free glutathione in the solution decomposed and lost its thiol group, forming a layer of CdS or $CdTe_xS_{1-x}$ on the QD. Hence, under the experimental condition, GSH could self-assemble on the QD to modify it and donor a negative charge on the surface of QD. The negatively charged GSH–CdTe QDs might bind to positively charged peptides [25,26]. Polymyxin B sulfate (PMBS, molecular structure given in Fig. 1(A)) is an antibiotic peptides. It is well-known that amino acid is composed of peptides. The buffer solution of Tris–HCl is used in the experiment to provide a protonation environment. As shown in the molecular structure (Fig. 1(A)), the $-NH_2$ groups in PMBS were connected to the peptide chain. Therefore, PMBS could be easily protonated and exist as the cation form in the neuter and weakly alkaline medium (Tris–HCl buffer solution, pH 7.2, 0.1 M) which was similar to physiological pH value [27]. On the basis of it, the negatively charged GSH-capped CdTe QDs and the positively charged PMBS could react to form the QDs–PMBS complex through electrostatic forces, resulting in the increase of the molecular volume and the enhancement of RRS intensity.

It could be seen from Fig. 6(A) that the RRS intensity of the separate PMBS solution (curve a) or the GSH-capped CdTe QDs solution (curve b) was very weak. When the QDs and PMBS were mixed together in Tris–HCl buffer solution (pH 7.2, 0.1 M), RRS intensity of the system significantly enhanced in the wavelength range of 220–700 nm and reached a maximum at 380 nm. In the meantime, the effect of ionic strength on the RRS intensity of GSH-capped CdTe QDs–PMBS system was studied by adding NaCl solution, for the reason that NaCl was considered as a good ionic strength adjustor. From Fig. 6(B), when the ionic strength was increasing the RRS intensity decreased but the intensity of fluorescence increased. According to the effect of ionic strength on RRS intensity and FL intensity, it could be speculated that electrostatic attraction played an important role in the reaction of GSH-capped CdTe QDs and PMBS [28].

When a QD received the excitation light, the electrons would be excited from its valence band to the conduction band, causing the excited electron and the oppositely charged "hole" attracted one another. Moreover, a photon could be emitted in the form of fluorescence because the excited electron recombined with the hole [29]. In the process of experiment, the introduced positively charged PMBS could act as a cationic electron acceptor. This static association of GSH-capped CdTe QDs with PMBS initiated ultrafast photoinduced electron transfer from the QDs to the electron acceptor (PMBS), preventing the normal recombination of the electron and hole in QDs and causing the fluorescence quenching of QDs [30]. Presumably, it could be obtained that PMBS worked as an excellent quencher for the fluorescent GSH-capped CdTe QDs via the electron transfer mechanism.

3.3. Optimization of the reaction conditions

3.3.1. Effect of the acidity

According to the previous reports, the pH value of solution has a great influence on the fluorescence of QDs [31]. During the experiment, Tris–HCl buffer solution was elected to create a physiological environment and control the acidity of the solution. The effect of Tris–HCl buffer solution acidity on the GSH-capped CdTe QDs–PMBS system was investigated from pH 7.0 to 8.0. Maximal fluorescent change of PMBS-induced the fluorescence quenching of GSH-capped CdTe QDs was obtained at pH of 7.2. Hence, the pH of the solution was set at 7.2 in order to achieve a low detection limit for hsDNA.

3.3.2. Effect of GSH-capped CdTe QDs concentration

Through fixing parameters of the concentration of PMBS and the pH constant while changing the concentration of GSH-capped CdTe QDs, the accompanying fluorescence diversification of QDs–

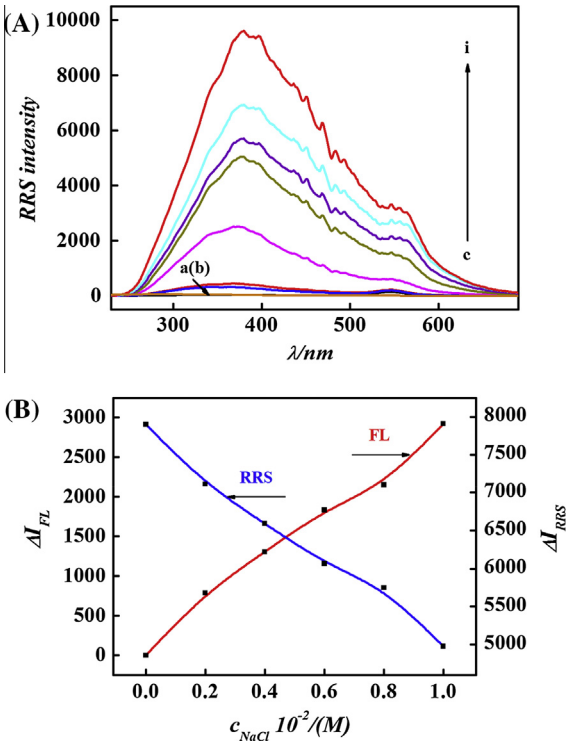

Fig. 6. (A) RRS spectra of GSH-capped CdTe QDs–PMBS system in Tris–HCl buffer solution (pH 7.2, 0.1 M), the concentration of PMBS was separately (μg mL^{-1}, curves b–i): 0, 2.0, 4.0, 6.0, 8.0, 10.0, 12.0 and 14.0, and the curve a represented the RRS spectrum of PMBS (10.0 μg mL^{-1}). (B) Effects of ionic intensity on the GSH-capped CdTe QDs–PMBS solution system in Tris–HCl buffer solution (pH 7.2, 0.1 M), (GSH-capped CdTe QDs, 2.0×10^{-4} M; PMBS, 14.0 μg mL^{-1}).

PMBS system was analyzed. Since the added concentration of GSH-capped CdTe QDs went beyond 2.0×10^{-4} M, the quenched fluorescence intensity of the system remained almost unchanged which was presumably for the reason that limited PMBS molecules could not occupy all the binding sites of QDs with higher concentrations, as shown in Fig. 7. This phenomenon indicated that the optimum concentration of GSH-capped CdTe QDs was 2.0×10^{-4} M.

3.3.3. Effect of incubation time

The effect of incubation time on the GSH-capped CdTe QDs–PMBS system under room temperature was studied. The results drawn from the analysis revealed that the reaction finished within 10 min and the fluorescence intensity of the system could remain almost unchanged within 60 min. Since the reaction reached a steady state after 10 min, the time scale of 10 min was chosen as the detection time throughout this experiment.

3.3.4. Effect of ionic strength

NaCl solution was found to be a good ionic strength adjustor and a stabilizer for the double helix structure of DNA. Therefore, the effects of ionic strength on the GSH-capped CdTe QDs–PMBS systems were investigated by adding NaCl solution and the experimental results exhibited that the system's RRS intensity decreased and FL intensity increased with increasing ionic strength (Fig. 6(B)). By analyzing the variation of the RRS intensity and the FL intensity in the reaction system with the in draught of NaCl solution, it could be demonstrated that low concentration of NaCl solution was not enough to stabilize the DNA structure and excessive concentration could lead to the enhancement of counterion separating the GSH-capped CdTe QDs and PMBS. In this case, this interaction should be under a certain ionic strength concentration, namely, the 0.005 M NaCl concentration should be added into the reaction system to decrease the disturbance of nonspecific substances to ensure the good selectivity of the detection system. The result demonstrated the electrostatic interaction was a significant and decisive factor in this ion-association reaction, as well.

3.4. HsDNA-induced fluorescence enhancement of GSH-capped CdTe QDs–PMBS system: "turn-on" pattern

As shown in Fig. 8(A), the increasing amounts of hsDNA added into the GSH-capped CdTe QDs–PMBS system led to the fluorescence enhancement of the solution. At the same time, a blue shift (9 nm) on maximum emission peak was observed (from 563 to 554 nm). However, in the controlled experiments, the fluorescence

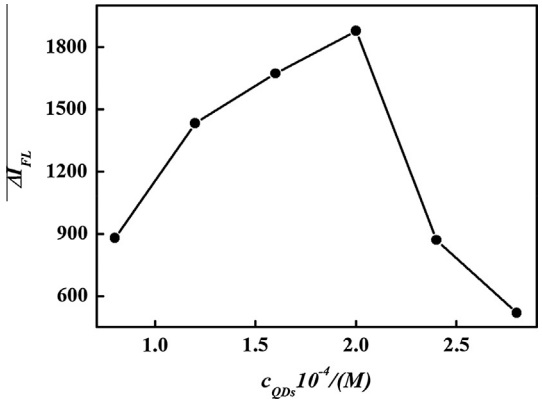

Fig. 7. Effect of the concentration of aqueous GSH-capped CdTe QDs on the quenched fluorescence intensity of the solution system in 0.1 M Tris–HCl buffer solution at pH = 7.2, (PMBS, 10 μg mL^{-1}).

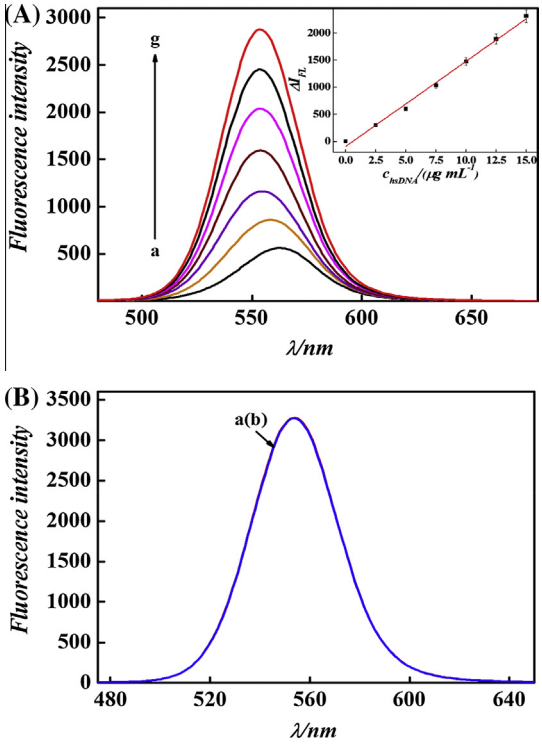

Fig. 8. (A) Fluorescence spectra of GSH-capped CdTe QDs–PMBS–hsDNA system in Tris–HCl buffer solution (pH 7.2, 0.1 M), the concentration of hsDNA was (μg mL^{-1}, curves a–g): 0, 2.5, 5.0, 7.5, 10.0, 12.5 and 15.0, separately; the inset revealed the relationship of the restored fluorescence intensity of the GSH-capped CdTe QDs–PMBS system with the concentration of hsDNA. (B) Fluorescence spectra of GSH-capped CdTe QDs in the absence (a) and presence (b) of hsDNA in Tris–HCl buffer solution (pH 7.2, 0.1 M), (GSH-capped CdTe QDs, 2.0×10^{-4} M; PMBS, 14.0 μg mL^{-1}; hsDNA, 10.0 μg mL^{-1}).

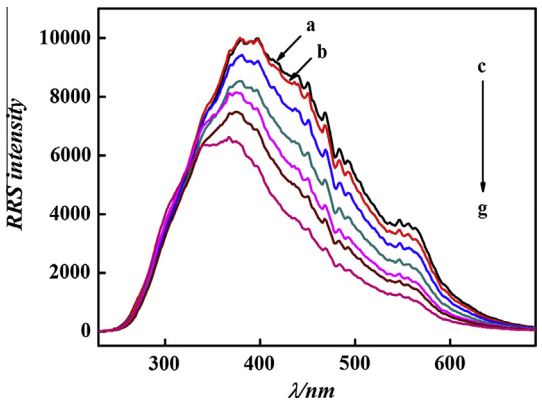

Fig. 9. RRS spectra of GSH-capped CdTe QDs with addition of 14.0 μg mL^{-1} PMBS restored due to the introducing of hsDNA in Tris–HCl buffer solution (pH 7.2, 0.1 M), the concentration of hsDNA was (μg mL^{-1}, curves a–g):0, 2.5, 5.0, 7.5, 10.0, 12.5 and 15.0, separately.

emission of GSH-capped CdTe QDs was not influenced by the direct addition of hsDNA, as displayed in Fig. 8(B). It could be inferred that the fluorescence restoring process was due to the interaction between PMBS and hsDNA.

Based on the above analyses, PMBS induced fluorescence quenching of GSH-capped CdTe QDs was attributed to the electron transfer mechanism which could be easily influenced by the distance between donor and acceptor. If the PMBS (acceptor) was far away from the GSH-capped CdTe QDs (donor), the excited electron could recombine with the hole and a photon in QDs could

emit in the form of fluorescence. Therefore, with the addition of hsDNA, PMBS could combine with hsDNA to generate a new complex and move away from the surface of GSH-capped CdTe QDs, resulting in the interruption of the electron transfer from QDs to PMBS. In the light of the fact that the maximum emission wavelength of GSH-capped CdTe QDs was returned to the original value (554 nm), the fluorescent QDs were set free in the above reaction process which propelled the fluorescence recovery of the QDs.

Generally, a variety of drug molecules interact with DNA are through three modes of intercalating, electrostatic attraction and groove binding. In this work, the RRS spectra of GSH-capped CdTe QDs–PMBS–hsDNA system were analyzed to investigate the interaction mechanism. As shown in Fig. 9, the RRS intensity of GSH-capped CdTe QDs–PMBS was gradually decreased with increasing amounts of hsDNA, indicating the complex of GSH-capped CdTe QDs–PMBS–hsDNA was not formed. It was good evidence that the interaction between hsDNA and PMBS was not electrostatic attraction or groove binding, as well [32]. It could be deduced from the above analyses that PMBS intercalated into hsDNA double helix structure and deviated from the surface of GSH-capped CdTe QD.

Absorption spectroscopy is an effective method for detecting DNA structural transitions and their interactions with micromolecules, which can obtained from the spectral features of hyperchromism and hypochromism [33]. While hyperchromism originates from the damage of the DNA doplex secondary structure, hypochromism is considered as the contraction of DNA in the helix axis. [34]. Therefore, UV–vis absorption measurement was performed to monitor the denaturation of the hsDNA duplexes in the presence and absence of PMBS at various concentrations under this experimental environment [35–37]. It was observed from Fig. 10(A) that the addition of PMBS to the hsDNA solution induced a strong hyperchromicity effect by comparing curve b and curve d. Considerable changes in UV–vis absorption spectra of PMBS upon interaction with hsDNA supported the viewpoint of the complex formation. As shown in Fig. 10(B), the maximium absorption peak as well as the characteristic absorption peak of hsDNA was located at 260 nm was increased in intensity with an obvious 7 nm red shift. The classical intercalative binding had been characterized by large changes in the absorbance (hyperchromism) and an obvious red shift in wavelength ($\leqslant$15 nm) [38–40]. As a consequence, the experimental results made it unambiguous that an intercalation binding actually existed between hsDNA and PMBS.

Namely, the PMBS embedded into hsDNA double helix structure to form more stable complex through intercalation and be dissociated from the surface of GSH-capped CdTe QDs. The fluorescence intensity of GSH-capped CdTe QDs could be recovered, on account that the electron transfer process between the QDs and PMBS was suppressed by the addition of hsDNA.

3.5. Fluorescence detection for hsDNA with the (QDs–PMBS)-based fluorescent biosensor

3.5.1. Analytical characteristics

In order to verify the sensitivity of the designed fluorescent biosensor which was based on the GSH-capped CdTe QDs–PMBS system, the fluorescence intensity of the QDs–PMBS system was investigated as a function of various concentrations of hsDNA in the experimental conditions. As shown in the inset of Fig. 8(A), the relationship between the restored fluorescence intensity and the different concentrations of hsDNA was linearly in the range of 0.059–15.0 μg mL^{-1}, which fitted the following regression equation: $\Delta F = 157.03c - 91.04$ (c: μg mL^{-1}). In the above relational expression, ΔF was the difference values of F (recovered fluorescence intensity) and F_0 (fluorescence intensity of GSH-capped CdTe QDs quenched by PMBS at the concentration of 14.0 μg mL^{-1}). This equation demonstrated a good linear correlation coefficient of 0.9937, the low limit of linear range (0.059 μg mL^{-1}) was calculated by 10 σ/K, and the detection limit for hsDNA was 0.018 μg mL^{-1} which was counted by 3 σ/K (where σ was the standard deviation for eleven blank samples been measured by experimental methods and K was the slope of the calibration plot).

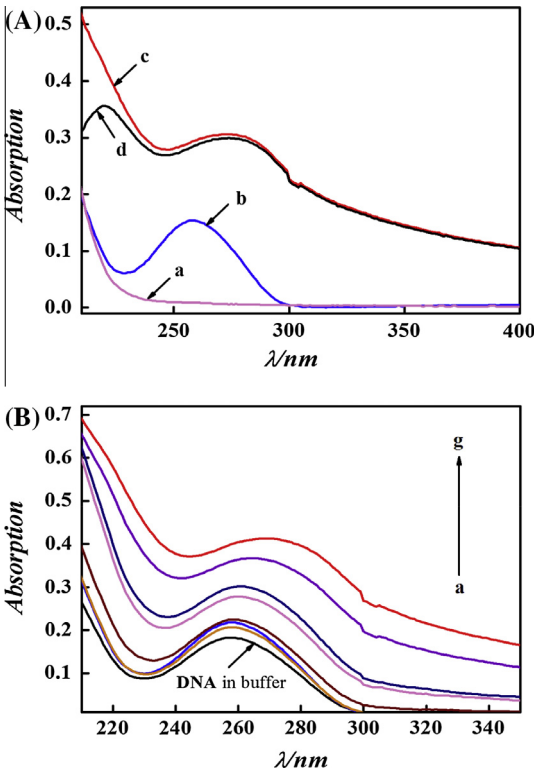

Fig. 10. (A) UV–vis absorption spectra of (a) PMBS (with distilled water as the reference), (b) hsDNA, (c) the mixture solution (PMBS and hsDNA), and (d) hsDNA (with PMBS as the reference) (PMBS, 14.0 μg mL^{-1}; hsDNA 10.0 μg mL^{-1}). (B) UV–vis absorption spectra of hsDNA with various concentrations of PMBS in Tris–HCl buffer solution (pH 7.2, 0.1 M). The concentration of hsDNA was 10.0 μg mL^{-1} and the concentration of PMBS was (μg mL^{-1}, curve a-g): 2.0, 4.0, 6.0, 8.0, 10.0, 12.0 and 14.0, separately.

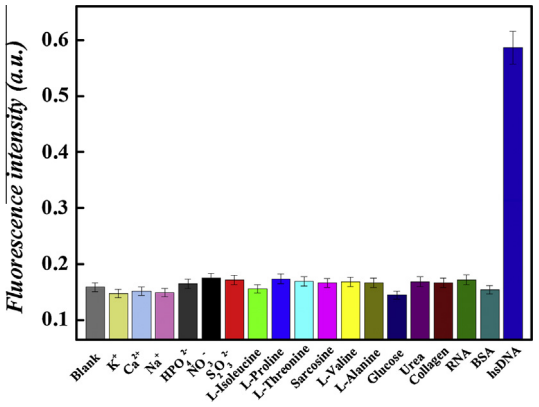

Fig. 11. The fluorescence responses of the GSH-capped CdTe QDs–PMBS system to different interferences in Tris–HCl buffer solution (pH 7.2, 0.1 M). Conditions: GSH-capped CdTe QDs, 2.0 × 10^{-4} M; PMBS, 14.0 μg mL^{-1}, hsDNA, 10.0 μg mL^{-1}; K^+, Na^+, HPO_4^{2-}, NO_3^-, $S_2O_3^{2-}$, 150 μg mL^{-1}; Ca^{2+}, 50 μg mL^{-1}; L-Cysteine, L-Isoleucine, L-Proline, L-Threonine, L-Tryptophan, L-Valine, L-Alanine, 200 μg mL^{-1}; glucose, urea, collagen, 200 μg mL^{-1}; RNA, 40.0 μg mL^{-1}; BSA, 20 μg mL^{-1}.

Table 2
Determination of hsDNA in synthetic samples.

Sample	Added ($\mu g\ mL^{-1}$)	Foreign substances ($\mu g\ mL^{-1}$)	Found ($\mu g\ mL^{-1}$)	Recovery ($n = 5\%$)	R.S.D. ($n = 5\%$)
1	10.0	KCl, $NaNO_3$, sarcosine, glucose	10.10	101.0	1.56
2	10.0	$CaCl_2$, Na_2SO_3, L-Threonine, urea	10.06	100.6	1.66
3	10.0	NaCl, Na_2HPO_4, L-Valine, collagen	9.93	99.3	1.89

3.5.2. Selectivity of the biosensor for hsDNA monitoring

To investigate the selectivity of this (QDs–PMBS)-based "turn off–on" fluorescent biosensor for hsDNA determining, a series of interferential experiments were carried out. A variety of biologically relevant chemical species such as ions, amino acid, organic compounds, hsDNA, RNA and BSA were introduced to the GSH-capped CdTe QDs–PMBS system (Fig. 11). The ions, including K^+, Ca^{2+}, Na^+, HPO_4^{2-}, NO_3^- and $S_2O_3^{2-}$, did not exhibit a significant effect on the fluorescence of the GSH-capped CdTe QDs–PMBS system. Amino acid, such as L-Cysteine, L-Isoleucine, L-Proline, L-Threonine, L-Tryptophan, L-Valine and L-Alanine, did not cause any interference to the biosensor. RNA which lacks the double helix structure of hsDNA could not specifically combine with PMBS and thus hardly had influence on the emission fluorescence of this biosensor, as well. Large protein molecules exemplified by BSA could be allowed at high concentration in the system without any obvious interference. Other organic matters, such as glucose, urea and collagen, had also been brought into the biosensor and the consequence illustrated that they have no prominent influence on it. The corresponding results demonstrated that only hsDNA could recover the fluorescence of the GSH-capped CdTe QDs–PMBS system and enable this (QDs–PMBS)-based fluorescent biosensor to be turn-on, implying good selectivity of the designed biosensor for monitoring hsDNA. Apparently, nonspecific binding that commonly associated with biosensor development was not a problem in this study.

3.5.3. Analytical applications

A series of detection experiments were implemented to evaluate analytical performance of this proposed (QDs–PMBS)-based fluorescent biosensor for detecting hsDNA in synthetic samples. The samples were containing inorganic salt, amino acid and organic compounds. As could be seen from Table 2, the recoveries (from 99.3% to 101%) of the added hsDNA were satisfactory and the relative standard deviations (R.S.D.) were less than 5.0%. Therefore, this (QDs–PMBS)-based "turn off–on" fluorescent biosensor was reliable and practical to be applied to the rapid monitoring of hsDNA.

4. Conclusions

A novel and sensitive biosensor for the determination of hsDNA which was based on fluorescent reversible "turn off–on" change of GSH-capped CdTe QDs had been established. With the introduction of PMBS, original fluorescence of GSH-capped CdTe QDs was markedly quenched which was ascribed to the occurrence of the photoinduced electron transfer from the QDs to PMBS. On account of the fact that PMBS could embed into hsDNA double helix structure to form more stable complex through intercalation and then dissociate from the surface of QDs, the fluorescence of GSH-capped CdTe QDs would be restored. This designed biosensor with a good linear correlation coefficient and a low detection limit exhibited a high sensitivity of hsDNA detection. Interferences caused by metal ions, inorganic anions, amino acid and organic matters hardly had effect on the determination of hsDNA, conforming the good selectivity of this biosensor. Concurrently, the proposed biosensor demonstrated a high sensitivity for detecting hsDNA in synthetic samples. These satisfying results also threw light on the prospective probability of investigating the interaction mechanism of antibiotics with DNA.

Acknowledgments

This work was supported by Chongqing Municipal Key Laboratory on Luminescence and Real-Time Analysis, Southwest University (CSTC, 2006CA8006) and the National Natural Science Foundation of China (No. 21175015).

References

[1] Y. Shi, C.L. Guo, Y.J. Sun, Z.L. Liu, F.G. Xu, Y. Zhang, Z.W. Wen, Z. Li, Biomacromolecules 12 (2011) 797–803.
[2] C. Tong, Z. Hu, W. Liu, Talanta 71 (2007) 816–821.
[3] A.E. Radi, A.E. El-Naggar, H.M. Nassef, Electrochim. Acta 129 (2014) 259–265.
[4] W. Zhang, Q.M. Chen, X. Cheng, N. Wu, G.B. Yi, D. Li, J.H. Tan, Z.S. Huang, L.Q. Gu, L.K. An, Dyes. Pigments 99 (2013) 82–89.
[5] C. Chen, B.X. Li, Biosens. Bioelectron. 54 (2014) 48–54.
[6] S. Shahrokhian, S. Rastgar, M.K. Amini, M. Adeli, Bioelectrochemistry 86 (2012) 78–86.
[7] A.H. Thomas, J.M. Thomas, I. Holloway, Analyst 105 (1980) 1068–1075.
[8] P. Srisom, B. Liawruangrath, S. Liawruangrath, J.M. Slater, S. Wangkarn, J. Pharm. Biomed. Anal. 43 (2007) 1013–1018.
[9] G.M. Durán, M.R. Plata, M. Zougagh, A.M. Contento, Áng. Ríos, J. Colloid Interface Sci. 428 (2014) 235–241.
[10] R.H. Yang, J.Y. Jin, Y. Chen, N. Shao, H.Z. Kang, Z.Y. Xiao, Z.W. Tang, Y.R. Wu, Z. Zhu, W.H. Tan, J. Am. Chem. Soc. 130 (2008) 8351–8358.
[11] S.S. Yang, C.L. Ren, Z.Y. Zhang, J.J. Hao, Q. Hu, X.G. Chen, J. Fluoresc. 21 (2011) 1123–1129.
[12] K. Hu, Y. Huang, S.E. Wang, S.L. Zhao, J. Pharm. Biomed. Anal. 95 (2014) 164–168.
[13] Q.Q. Wang, G.Q. Zhan, C.Y. Li, Spectrochim. Acta Part A Mol. Biomol. Spectrosc. 117 (2014) 198–203.
[14] X.F. Li, J. Li, H.Y. Kuang, L. Feng, S.J. Yi, X.D. Xia, H.W. Huang, Y. Chen, C.R. Tang, Y.L. Zeng, Anal. Chim. Acta 802 (2013) 82–88.
[15] S.J. He, B. Song, D. Li, C.F. Zhu, W.P. Qi, Y.Q. Wen, L.H. Wang, S.P. Song, H.P. Fang, C.H. Fan, Adv. Funct. Mater. 20 (2010) 453–459.
[16] E.M. Nolan, S.J. Lippard, Chem. Rev. 108 (2008) 3443–3480.
[17] Y.F. Liu, J.S. Yu, J. Colloid Interface Sci. 333 (2009) 690–698.
[18] Z.Q. Liu, S.P. Liu, P.F. Yin, Y.Q. He, Anal. Chim. Acta 745 (2012) 78–84.
[19] C. Würth, M.G. González, R. Niessner, U. Panne, C. Haisch, U.R. Genger, Talanta 90 (2012) 30–37.
[20] B.H. Dong, L.X. Cao, G. Su, W. Liu, H. Qu, D.X. Jiang, J. Colloid Interface Sci. 339 (2009) 78–82.
[21] Y.M. Liu, H.H. Li, M.S. Pei, G.Y. Zhang, L.L. Hu, J.T. Han, Talanta 115 (2013) 190–194.
[22] X.L. Li, Y.J. Hu, H. Wang, B.Q. Yu, H.L. Yue, Biomacromolecules 13 (2012) 873–880.
[23] J.R. Lakowicz, Principles of Fluorescence Spectroscopy, third ed., Springer Science Business Media, New York, 2006.
[24] S.P. Liu, Z. Yang, Z.F. Liu, J.T. Liu, Y. Shi, Anal. Chim. Acta 572 (2006) 283–289.
[25] M.T. Fernández-Argüelles, J.M. Costa-Fernández, R. Pereiro, A. Sanz-Medel, Analyst 133 (2008) 444–447.
[26] Y.G. Zheng, S.J. Gao, J.Y. Ying, Adv. Mater. 19 (2007) 376–380.
[27] T.S. Li, S.P. Liu, Z.F. Liu, X.L. Hu, L.P. Zhang, Sci. China Ser. B – Chem. 52 (2009) 76–85.
[28] J.J. Peng, S.P. Liu, L. Wang, Z.W. Liu, Y.Q. He, J. Colloid Interface Sci. 338 (2009) 578–583.
[29] D. Zhao, W.H. Chan, Z.K. He, T. Qiu, Anal. Chem. 81 (2009) 3537–3543.
[30] V.I. Klimov, J. Phys. Chem. B 104 (2000) 6112–6123.
[31] S.H. Fu, Z.F. Liu, S.P. Liu, A.E. Yi, Talanta 75 (2008) 528–535.
[32] L.L. Zhao, X. Wu, H.H. Ding, J.H. Yang, Analyst 133 (2008) 896–902.
[33] C.Y. Zhou, X.X. Li, P. Yang, Biochemistry 72 (2007) 37–43.
[34] Q.S. Li, P. Yang, H.F. Wang, M.L. Guo, J. Inorg. Biochem. 64 (1996) 181–195.
[35] S.S. Kalanur, U. Katrahalli, J. Seetharamappa, J. Electroanal. Chem. 636 (2009) 93–100.
[36] W.C. Tse, D.L. Boger, Chem. Biol. 11 (2004) 1607–1617.
[37] G. Psomas, J. Inorg. Biochem. 102 (2008) 1798–1811.
[38] A.E. Friedman, J.C. Chambron, J.P. Sauvage, N.J. Turro, J.K. Barton, J. Am. Chem. Soc. 112 (1990) 4960–4962.
[39] Y.J. Guo, J.B. Chao, J.H. Pan, Spectrochim. Acta A 68 (2007) 231–236.
[40] X.Q. Liu, R. Aizen, R. Freeman, O. Yehezkeli, I. Willner, ACS Nano 6 (2012) 3553–3563.